Crystal Structure and Adjacent Reentry Folds of the α Form of Syndiotactic Polystyrene. Conformational and Packing Analysis by Molecular Mechanics

Roberto Napolitano and Beniamino Pirozzi*

Dipartimento di Chimica, Università di Napoli Federico II, Complesso Universitario Monte S. Angelo, via Cintia, 80126 Napoli, Italy

Received October 14, 2002; Revised Manuscript Received December 20, 2002

ABSTRACT: The crystal structure of the ordered α form of syndiotactic polystyrene and the adjacent reentry folds of the polymer chains have been analyzed by molecular mechanics adopting various set of potential functions. The energy calculations indicate that the crystal structure is well described by the *P*3 space group, in accordance with the experimental crystal structure recently reported. The energy required to fold the polymer chains has been optimized by taking into account both the conformational energy of the folds and the interactions between the atoms of the folds and the atoms of the crystal. The work of fold evaluated for the α form is very similar to that previously calculated for the *β* form, suggesting that the chain folding of syndiotactic polystyrene is regulated by the conformation and configuration of the chains rather than by their modes of packing.

Introduction

Since highly stereoregular syndiotactic polystyrene (sPS) has been synthesized,[1−3] it has been studied by various authors who have evidenced its complex polymorphism. In fact, sPS crystallizes in various crystalline polymorphic forms, some mesophases/submodifications differing for the conformation of the polymer chain and some others for the mode of packing of chains having the same conformation.[4−7] In particular, the chains have a nearly trans planar conformation in the two crystalline forms indicated as α and *β*, and a 2-fold helical conformation in the other forms, indicated as *γ* and *δ*. Moreover, various clathrate forms also having the chains in a 2-fold helical conformation have been characterized.

The α and *β* form can be obtained by crystallization from the melt at high and low supercooling, respectively. Also, depending on the crystallization conditions, various crystalline modifications corresponding to different degrees of order have been found for both forms. All the structural data of the α form evidence that the chains are arranged in triplets around 3-fold symmetry axes parallel to the chain axes.[8−12] The triplets are characterized by an inner core with chain backbones at van der Waals contact and by phenyl rings at the periphery. The *β* form crystallizes in an orthorhombic unit cell characterized by bilayers along the *a* direction.[13,14] The bilayers are constituted by chains related by 2-fold symmetry axes parallel to the *c* axis, according to the $P2_12_12_1$ space group proposed for the completely ordered modification, or by 2-fold axes parallel to the *c* axis and mirror planes perpendicular to the *a* axis, according to the *Cmcm* space group proposed for the completely disordered modification.

The clathrate forms can be obtained by swelling samples of the α form in various solvents and by subsequent removal of the solvents.[4,5,15] The *γ* form can be obtained by annealing the clathrate forms, while the *δ* form can be obtained by suitable solvent extraction procedures on samples of the clathrate forms.[4,5,15,16] The crystal structures of three clathrate forms, as well as of the *δ* form, have been reported.[16−19] A complete crystal structure of the *γ* form has not been reported until now.

The crystal structure of the α form was first determined by Greis et al.[8] as a result of high-energy electron diffraction studies. They proposed for the ordered modification a hexagonal unit cell with $a = 26.25$ Å and $c = 5.045$ Å, containing enantiomorphous triplets with the heights of the phenyl rings fixed by the symmetry elements of the *P*62*c* space group. Subsequently, De Rosa et al.[9] proposed for the ordered modification the trigonal *P*3*c*1 space group in which all the chains are crossed by glide planes, the triplets are rotated by 30° with respect to the previous structure, and the heights of the three independent triplets are shifted by $^1/_3$. In the same paper the authors proposed for the disordered modification the $R\bar{3}c$ space group, corresponding to the statistical occurrence of two different, nearly isosteric orientations of the triplets whose chains are still crossed by glide planes. Subsequently, packing energy calculations[10] showed that a rotation by 7° of the triplets around their axes gives a better mode of packing of the chains in the disordered crystal modification. In a further paper, De Rosa[11] suggested a rotation by 7° of the triplets with respect to the glide plane of the *P*3*c*1 space group also for the ordered modification, better described by the *P*3 space group. Finally, Cartier et al.[12] reevaluated the crystal structure of the ordered modification, pointing out its frustrated character and confirming the *P*3 space group but finding that a better accordance with the electron diffraction data was obtained with different values of the rotation angles of the three independent triplets.

Morphology and crystallization of the α form, also correlated to the transition to the more stable *β* form, were examined by various authors.[20−23] These studies, performed using various experimental techniques, were aimed to understand the main characteristics of the spherulitic or lamellar morphology and the relationships between morphology, unit cell crystal forms, and thermal behavior in cold-crystallized sPS. Recently,[24] in

10.1021/ma021588s CCC: $25.00
Published on Web 01/30/2003

order to investigate the fold direction, the lamellae were decorated with PE fragments, and no obvious preferred growth orientation of the decorated crystal rods was observed on the lamellar surfaces.

In this paper we report the results of molecular mechanics analysis of the crystal structure and of the possible models of adjacent reentry chain folding of the α form of sPS performed using various force fields. The internal energy of the crystalline ordered α modification has been optimized in order to find the best internal parameters of the chains and space group. The models of adjacent reentry folds have been found and optimized by conformational and packing energy calculations in order to find the best conformational parameters of the folds. The internal energy values of the folds have been used to estimate the work of fold. Energy calculations of adjacent reentry folds taking also into account the packing of the chains have been performed in the past for polyethylene[25−27] and recently by us for syndiotactic polypropylene,[28] poly(*p*-phenylene sulfide),[29] and the *β* form of sPS.[30] This work presents a more complete analysis of the influence of the crystalline field on the folds for a polymer with crystal structure more complex than those studied in the past.

Method of Calculation

All the calculations of the internal energy and of the diffraction spectra were performed using the Cerius[2] program by Accelrys. The crystals were generated by the Crystal Builder module. Starting from the crystal and removing the symmetry elements, we built up the models of fold connecting two chosen chains in appropriate way. The energy was minimized using the Open Force Field module by the smart minimizer method with standard convergence. The following force fields were used: Universal1.02,[31] UFF_Valbond,[32] Dreiding,[33] MM2_85,[34] and Compass.[35] The electrostatic term was calculated for all the force fields with the exception of MM2_85. According to the suggestions of the authors, the electrostatic charges were calculated by the charge equilibration method[36] in the use of Universal1.02 and UFF_Valbond, while Gasteiger[37] estimates for charges were taken into account in the use of Dreiding. The Compass force field has its own method of calculation of the electrostatic charges. The Analytical module was used to calculated the X-ray and electron diffraction spectra.

Crystal Structure of the Ordered Modification

As reported above, the main structural feature of the α form of sPS is the occurrence of triplets that are clusters constituted by three chains related by 3-fold symmetry axes parallel to the *c* axis. We have characterized the closeness of the chains within a triplet by the parameter *d* which represents the distance between the carbon atoms of the methylene groups at the same height belonging to two chains. We have first examined the best arrangement of the chains inside the triplet with the various set of potential functions. To obtain the internal energy of a single triplet, the triplet has been generated by positioning a chain around a 3-fold axis of a unit cell in the *P*3 space group using a very high value (100 Å) of the *a* (=*b*) axis. In this way, the atoms of different triplets are very far and their interactions are negligible. The energy minimizations performed with all force fields give chain conformations which can be ascribed to the *tcm* line repetition group.[38]

Table 1. Values of the Torsion Angle θ (deg) and of the Bond Angles τ_{CH} and τ_{CH_2} (deg) of the Backbone, of the Chain Axis *c*, and of the Distance d_0 between the Carbon Atoms of the Methylene Groups at the Same Height Belonging to Two Chains of the Triplet Obtained by the Minimizations of the Internal Energy of a Single Triplet with the Various Force Fields

	Universal 1.02	UFF_Valbond	Dreiding	MM2_85	Compass
θ	168	167	168	173	172
τ_{CH}	110.6	112.3	113.0	112.1	113.2
τ_{CH_2}	111.7	113.7	114.1	112.4	113.6
c/Å	5.08	5.11	5.22	5.11	5.16
d_0/Å	4.26	4.26	4.36	4.16	4.12

Table 1 shows the optimized values of the independent parameters of the main chain (i.e., the torsion angle θ and the bond angles τ_{CH} and τ_{CH_2}), of the chain axis *c*, and of the optimized value d_0 of the previously defined parameter *d*. The conformational parameters found by the MM2_85 force field are very close to those previously obtained[6] by minimization of the isolated chain under the constraint of the *tcm* line repetition group.

Subsequently, we have taken into account not only the interactions between the atoms inside a triplet but also the interactions between atoms of neighboring triplets. To this end, we have minimized the energies imposing the experimental value of the *a* axis of the unit cell in the space groups proposed by the various authors[8,11,12] for the ordered α form. They are $P\bar{6}2c$, *P*3*c*1, and *P*3, which have two, three, and three independent triplets, respectively. In the $P\bar{6}2c$ space group the triplets can neither rotate around their 3-fold axes nor translate along the *c* direction, due to symmetry planes. In the *P*3*c*1 space group the position of the chains around the 3-fold axes are fixed, though rotated by 30° with respect to their position in the $P\bar{6}2c$ space group, but the translation along *c* is free. In the *P*3 space group the triplets are free both to rotate and to translate along *c*. The minimizations have been carried out for each force field under the restraints of maintaining inside all the triplets the parameter d_0 found in the minimizations of the isolated triplets. The restraints are imposed as harmonic potentials whose contributions are to be minimized together with all other force field contributions. The values of the restraining energy $E_{res} = {}^1/_2K(d - d_0)^2$, with *K* an arbitrary constant, are subtracted by the obtained values of the minimized energy. We have observed that, even if a high value of *K* is used, the exact value of d_0 is never obtained for the *P*3*c*1 space group, whatever the force field, and for the *P*3 space group for the Dreiding force field. In these cases, the minimizations have been halted when a value of *d* within 0.1 Å from the required value of d_0 had been obtained. After these minimizations, for each force field and for each space group, the conformations of chains belonging to independent triplets are practically equal. We have found that the values of the bond and torsion angles obtained by minimization in the *P*3 space group are very similar to those found by minimization of the isolated triplet for each force field. In the $P\bar{6}2c$ space group the t*cm* symmetry of the chain is crystallographic, but the values of bond and torsion angles increase with respect to those of the isolated triplet for each force field. For the *P*3*c*1 space group only the crystallographic t*c* symmetry of the chain is maintained, and consecutive independent backbone torsion angles assume substantially different values. As a consequence of the different values of the internal parameters, the *c* axis assumes

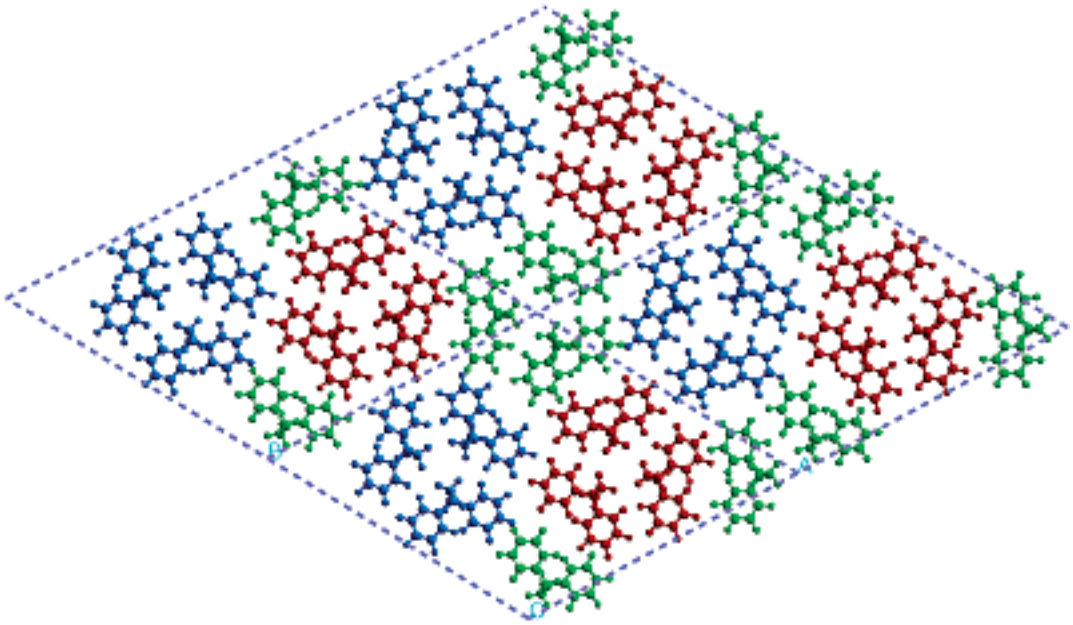

Figure 1. Projection along the *c* axis of the crystal structure of the ordered α form of sPS obtained by energy minimization with the MM2_85 force field. The content of four unit cells is reported. The three independent triplets are represented by three different colors.

Table 2. Values of the Energy *E* (kJ/mol of Monomeric Unit) and of the Chain Axis *c* (Å) Obtained by the Minimizations of the Internal Energy in the Considered Space Groups with the Various Force Fields

space group		Universal 1.02	UFF_Valbond	Dreiding	MM2_85	Compass
$P\bar{6}2c$	*E*	20.1	18.2	70.1	−18.8	−44.0
	c	5.17	5.23	5.33	5.13	5.17
*P*3*c*1	*E*	10.9	8.3	63.3	−19.7	−42.0
	c	5.06	5.06	5.21	5.08	5.14
*P*3	*E*	3.62	−1.4	58.4	−21.6	−43.8
	c	5.08	5.12	5.23	5.08	5.15

different values in the different space groups. Table 2 shows the optimized energies and *c* axes obtained for the considered force field and space groups. The values of the energy decrease from the $P\bar{6}2c$ to the *P*3 space group for all force fields, except for Compass for which the energy values of the $P\bar{6}2c$ and *P*3 space groups are almost equal and slightly lower with respect to the *P*3*c*1 space group. The values of *c* are in better accordance with the experimental value in the case of the *P*3*c*1 and *P*3 space groups for all the force fields. In any case the values of *c* calculated with the Dreiding force field are significantly higher with respect to the experimental value.

Our calculations lead to the conclusion that the crystal structure of the ordered α form of sPS having the lowest energy is realized in the *P*3 space group. The internal parameters of the chain and the structural parameters calculated by the MM2_85 force field are in very good agreement with those reported in previous papers.[6,39] Figure 1 shows a projection along the *c* axis of the crystal structure obtained by energy minimization with the MM2_85 force field. Figure 2 shows the corresponding calculated X-ray powder and single-crystal electron diffraction spectra. They are very similar to the experimental spectra.[9,12] Both the internal parameters and the mode of packing of the chains in the crystal structure of Figure 1 are in very good agreement with those reported by Cartier et al.[12] Therefore, we have considered this crystal structure in the following calculations of the models of fold.

Adjacent Reentry Folds: Geometry and Energy

The adjacent reentry fold has been examined considering models of fold obtained by connecting all the pairs of adjacent chains which have different geometrical relationships in the crystal structure of the α form of sPS, in such a way to characterize all possible paths of the folded chains. We have first considered the folds inside the triplet, in which only one kind of path of the folded chain is to be taken into account, since independent triplets are substantially equivalent. On the contrary, many paths between chains of different triplets are to be taken into account due to the different azimuthal orientations of the three independent triplets. Figure 3 shows a schematic representation of all the possible kinds of folds.

The study of the chain folding by molecular mechanics requires both a geometry and an energy analysis. In fact, the folded polymer chains have to fulfill the following conditions: (i) the atoms must assume the crystallographic positions when the chains reenter the crystal; (ii) the atoms of the folds must not give strong repulsive interactions both between themselves and with the atoms of the crystal. We have considered a folded polymer chain as constituted by an initial stem (hereafter starting stem) having regular conformation and belonging to the crystal, a central portion having nonregular conformation (the fold), and a final stem (hereafter end stem) having regular conformation re-entering the crystal. We have assumed as fold surface a "*quasi*-planar" surface perpendicular to the chain axes and crossing the carbon atoms of the methylene groups

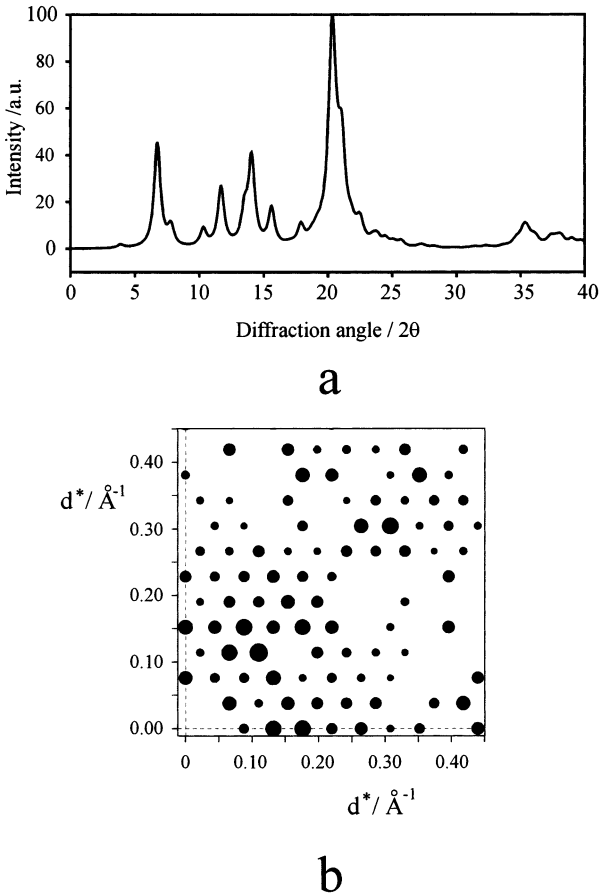

Figure 2. Calculated X-ray powder (a) and single-crystal electron diffraction (b) spectra of the ordered α form of sPS.

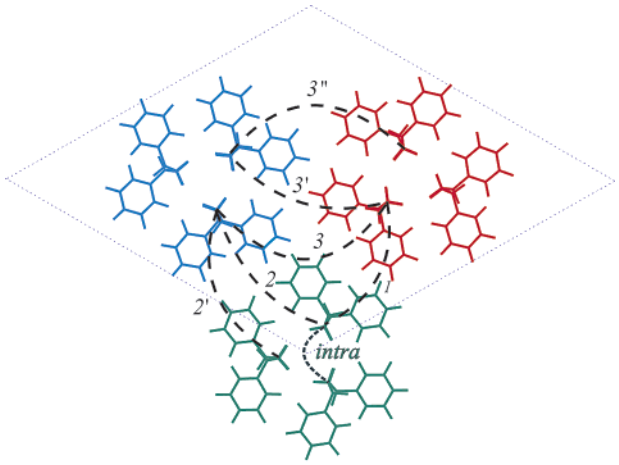

Figure 3. Schematic representations of all the possible folds (dashed lines). The term *intra* represents the fold connecting chains of the same triplet, while the numbers represent the folds connecting chains belonging to different triplets.

which are at the same height for chains of the same triplet and roughly at the same height for chains of different triplets. In this way, the atoms below this surface or lying on it have been fixed in the crystallographic positions, while the atoms above this surface have been considered to belong to the fold.

Each model of fold (hereafter starting model) has been built up in the following way: (i) a portion of crystal large enough to surround the two adjacent chains to be connected by the fold has been generated; (ii) the portion of the crystal has been cut along the fold surface leaving uncut the two chosen chains; (iii) two backbone atoms of the two portions of chains protruding out of the crystal have been connected in such a way that the generated folded chain had regular constitution and configuration. The regularity of the configuration requires that, for the found crystal structure and for the chosen fold surface, the folds connecting chains of the same triplet and the folds of kind 1 (see Figure 3) are constituted by an even number of monomeric units, while the folds of kind 2 and 3 are constituted by an odd number of monomeric units.

The starting models have been optimized (hereafter they are named optimized folds) taking into account all the interactions inside the folds and the interactions between the atoms of the folds and the atoms of the crystal. The interactions between atoms belonging to different folds have not been considered. We think, in fact, that, as verified in some cases, the conformations of the folds are not strongly affected by the neighboring folds in the crystal structure of the α form of sPS. On the other hand, considering that the unit cell contains three independent triplets of chains, many arrangements of the paths of fold on the fold surface are possible so that an exhaustive analysis would be very complex.

The energy has been calculated by using all the set of potential functions already adopted in the analysis of the crystal structure. For each fold sketched in Figure 3 we have built up and optimized models having different lengths. Each optimized fold has been refined (hereafter they are named refined folds) by a further minimization in which also the atoms of the two monomeric units close to the fold surface, one of the starting and one of the end stem, are allowed to move from the crystallographic positions. In this way the starting and the end stems enter the crystal gradually, in such a way that possible strong repulsive interactions between atoms of the fold and of the crystal can be relaxed.

After each minimization we have isolated the folded chain and calculated, for each force field, the conformational energy E_{conf} due to the interactions inside the fold and to the nonbonded interactions between the atoms of the fold and the atoms of the starting and end stems. We have evaluated the energy required to fold a chain, that is, the work of fold, as $E_{fold} = E_{conf} - E_{ref}$ where E_{ref} is, for each force field, the energy of an isolated chain having the same conformation of the polymer chain in the crystal and the same length of the fold.

Adjacent Reentry Folds: Results and Discussion

We have first tried models of fold for the path indicated as *intra* in Figure 3. As already discussed, these models of fold are constituted by an even number of monomeric units. We have found that folds consisting of four monomeric units are more suitable, because folds having two monomeric units are excessively strained and folds having six or more monomeric units are of high steric encumbrance. We have built up three starting models connecting chains having the same height (fold *intra*41), having heights which differ by two monomeric units (fold *intra*42), and having heights which differ by four monomeric units (fold *intra*43). Table 3 shows the values of E_{fold} of the optimized and refined folds *intra* obtained by all set of potential functions. The optimized fold *intra*43 is the lowest in energy, but the energy of the fold *intra*41 is only slightly

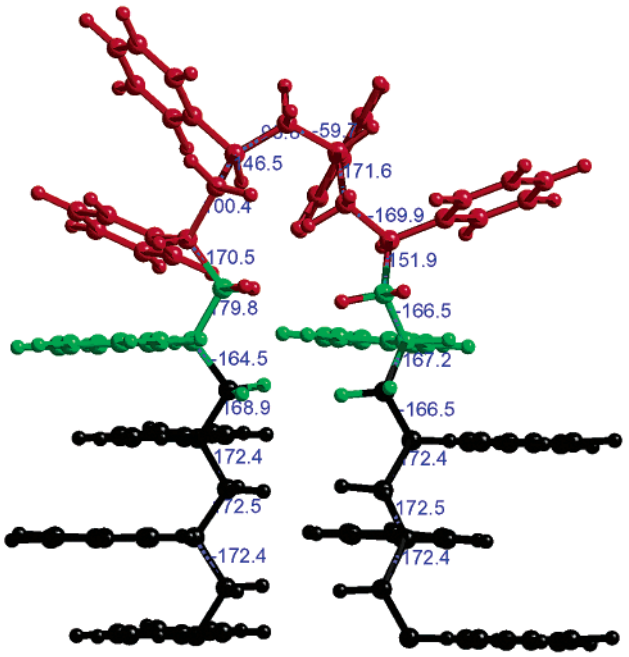

Figure 4. Projection in a plane parallel to the *c* axis of the refined fold *intra*43 obtained by the MM2_85 force field, with the indication of the values of the torsion angles of the backbone. The atoms of the fold, the atoms of the monomeric units of the starting and of the end stems nearer the fold surface, and the other atoms of the crystal are drawn with red, green, and black color, respectively.

Table 3. Values of E_{fold} (kJ/mol of Monomeric Unit) of the Optimized and Refined Folds *Intra* Calculated by the Indicated Force Fields

fold	Universal 1.02	UFF_Valbond	Dreiding	MM2_85	Compass
		Optimized			
*intra*41	162.2	108.6	129.2	71.0	71.2
*intra*42	165.6	135.2	141.2	81.7	86.2
*intra*43	140.1	103.8	126.1	63.3	61.4
		Refined			
*intra*41	102.8	74.0	114.5	56.3	60.8
*intra*42	136.7	101.6	126.1	65.1	84.5
*intra*43	102.8	72.3	109.6	55.9	58.3

higher. The corresponding refined folds are almost isoenergetic, and their conformations are very similar. The fold *intra*42 remains the highest in energy also in the refined model. Even if the energy differences of various models are quite different for the various force fields, the conclusions reported above are in all cases the same. Figure 4 shows a projection in the fold plane of the refined fold *intra*43 obtained by the MM2_85 force field, with the indication of the values of the torsion angles of the backbone.

We have successively tried starting models of fold for the path indicated as *1* in Figure 3. Also, these models of fold are constituted by an even number of monomeric units. We have found that the best folds have six monomeric units. We have built up three starting models connecting chains having the same height (fold *1*61), having heights which differ by two monomeric units (fold *1*62), and having heights which differ by four monomeric units (fold *1*63). Table 4 shows the values of E_{fold} of the optimized and refined folds *1* obtained by all set of potential functions. The optimized folds *1*61 and *1*63 are lower in energy with respect to the fold *1*62. The refined folds *1*61 and *1*63, lower in energy with respect to the refined fold *1*62, are almost isoenergetic,

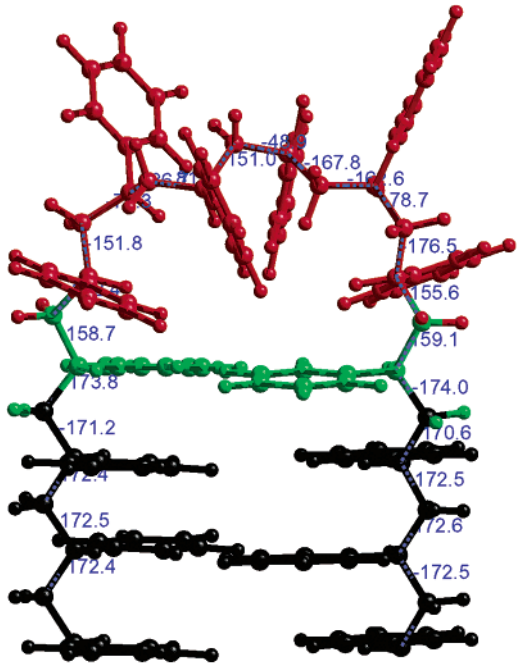

Figure 5. Projection in a plane parallel to the *c* axis of the refined fold *1*63 obtained by the MM2_85 force field, with the indication of the values of the torsion angles of the backbone. The atoms of the fold, the atoms of the monomeric units of the starting and of the end stems nearer the fold surface, and the other atoms of the crystal are drawn with red, green, and black color, respectively.

Table 4. Values of E_{fold} (kJ/mol of Monomeric Unit) of the Optimized and Refined Folds *1* Calculated by the Indicated Force Fields

fold	Universal 1.02	UFF_Valbond	Dreiding	MM2_85	Compass
		Optimized			
*1*61	118.9	100.4	107.5	74.9	80.8
*1*62	128.2	141.2	120.0	124.9	163.0
*1*63	83.6	67.5	106.4	75.4	78.4
		Refined			
*1*61	63.2	64.5	94.6	41.3	60.0
*1*62	89.4	111.8	85.9	101.2	76.6
*1*63	57.9	50.0	89.3	43.5	59.4

even if they correspond to different conformations. Figure 5 shows a projection in the fold plane of the refined fold *1*63 obtained by the MM2_85 force field, with the indication of the values of the torsion angles of the backbone.

As far as the remaining paths are concerned, two kinds of folds, indicated as *2* and *2′* in Figure 3, are possible for the path *2* and three kinds of folds, indicated as *3*, *3′*, and *3″* in Figure 3, are possible for the path *3*. All these folds are characterized by an odd number of monomeric units. As the pairs of chains connected by the fold *2* and *2′* have an almost equivalent relative positioning, we have studied models for the fold *2* only. In this case, we have found that good models can be obtained both for folds constituted by five monomeric units and for folds constituted by seven monomeric units. In both cases we have built up two starting models connecting chains having heights which differ by one monomeric unit (fold *2*51 and fold *2*71) and by three monomeric units (fold *2*52 and fold *2*72), respectively. Table 5 shows the values of E_{fold} of the optimized and refined folds *2* obtained by all the set of potential functions. The fold *2*72, which is a good optimized model,

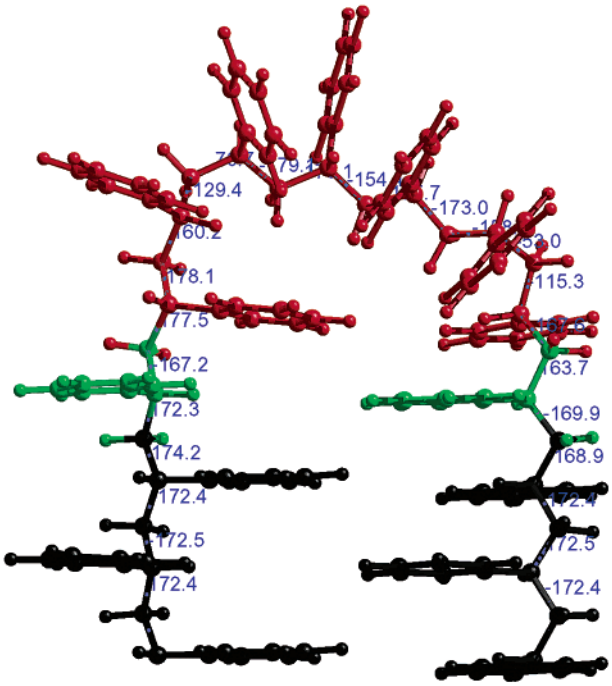

Figure 6. Projection in a plane parallel to the *c* axis of the refined fold *2*′*2* obtained by the MM2_85 force field, with the indication of the values of the torsion angles of the backbone. The atoms of the fold, the atoms of the monomeric units of the starting and of the end stems nearer the fold surface, and the other atoms of the crystal are drawn with red, green, and black color, respectively.

Table 5. Values of E_{fold} (kJ/mol of Monomeric Unit) of the Optimized and Refined Folds *2* Calculated by the Indicated Force Fields

	Universal 1.02	UFF_Valbond	Dreiding	MM2_85	Compass
			Optimized		
*2*51	171.1	136.7	146.0	74.5	97.6
*2*52	204.7	153.6	136.0	99.1	100.7
*2*71	117.2	80.0	116.1	77.5	93.3
*2*72	142.7	115.8	100.1	70.5	90.0
			Refined		
*2*51	124.7	109.7	88.3	47.4	77.4
*2*52	120.2	109.8	88.6	54.6	78.2
*2*71	107.5	75.3	112.0	69.9	88.1
*2*72	90.9	72.1	82.0	46.8	58.7

but not the best for all the set of potential functions, becomes the best in all cases after refinement. Figure 6 shows a projection in the fold plane of the refined fold *2*′*2*, obtained by the MM2_85 force field, with the indication of the values of the torsion angles of the backbone.

Finally, we have examined the path *3*, taking into account the folds *3* and *3*′, since the pairs of chains connected by the folds *3* and *3*″ are in an almost equivalent relative positioning. In both cases we have found that the best models are obtained for folds constituted by seven monomeric units. Both for the fold *3* and for the fold *3*′ we have built up three starting models: one model connecting chains with heights differing by one monomeric unit (fold *3*71 and fold *3*′71), one model connecting chains with heights differing by three monomeric units (fold *3*72 and fold *3*′72), and one model connecting chains with heights differing by five monomeric units (fold *3*73 and fold *3*′73). Table 6 shows the values of E_{fold} of the optimized and refined folds *3* obtained by all set of potential functions. As far as the optimized folds are concerned, the fold *3*73 is by far the best model and the fold *3*72 is lower in energy with respect to the fold *3*71, for all set of potential functions. The sequence of the energy values of the corresponding refined models remains the same, but the differences of the energy values are in all cases lower. Figure 7 shows a projection in the fold plane of the refined fold *3*73 obtained by the MM2_85 force field, with the indication of the values of the torsion angles of the backbone. Table 7 shows the values of E_{fold} of the optimized and refined folds *3*′ obtained by all the set of potential functions. The three optimized folds calculated by MM2_85 and Compass are practically isoenergetic, while controversial energy results are obtained by calculations with the other set of potential functions. Controversial results are also obtained by calculations of the refined folds. Nevertheless, the overall results give in this case the indication that the fold *3*′72 should be preferred. Figure 8 shows a projection in the fold plane of the refined fold *3*′72 obtained by the MM2_85 force field, with the indication of the values of the torsion angles of the backbone.

Table 6. Values of E_{fold} (kJ/mol of Monomeric Unit) of the Optimized and Refined Folds *3* Calculated by the Indicated Force Fields

	Universal 1.02	UFF_Valbond	Dreiding	MM2_85	Compass
			Optimized		
*3*71	156.8	107.9	114.9	67.4	90.2
*3*72	139.8	102.9	112.4	59.3	84.6
*3*73	102.7	80.3	88.2	52.6	61.5
			Refined		
*3*71	127.1	95.0	106.8	62.4	82.3
*3*72	118.6	84.3	99.7	52.7	65.9
*3*73	99.5	76.9	88.2	51.2	56.0

Table 7. Values of E_{fold} (kJ/mol of Monomeric Unit) of the Optimized and Refined Folds *3*′ Calculated by the Indicated Force Fields

	Universal 1.02	UFF_Valbond	Dreiding	MM2_85	Compass
			Optimized		
3′71	121.1	80.6	102.8	56.0	81.3
3′72	116.0	87.3	101.7	56.5	81.8
3′73	151.3	120.5	93.5	56.2	82.0
			Refined		
3′71	80.4	57.4	89.6	42.3	66.3
3′72	89.9	70.5	78.9	35.4	61.7
3′73	136.5	112.2	87.0	48.0	66.9

Conclusions

The results of the calculations performed by molecular mechanics with various force fields indicate that the *P*3 space group is best suited to describe the crystal structure of the ordered α form of sPS, in accordance with experimental results.[12] A detailed analysis of the structural parameters, including the internal parameters of the polymer chains, obtained with the various force fields leads to the conclusion that MM2_85 and Compass give results in better accordance with the experimental data, and therefore these force fields seem more adequate to deal with this polymer.

The analysis of the models of fold reported in this paper is particularly elaborate because it takes into account not only the interactions between the atoms of the folds and the atoms of the crystal as performed for the *β* form of sPS[30] but also gradual adjustments of the chains reentering the crystal, as calculated in the

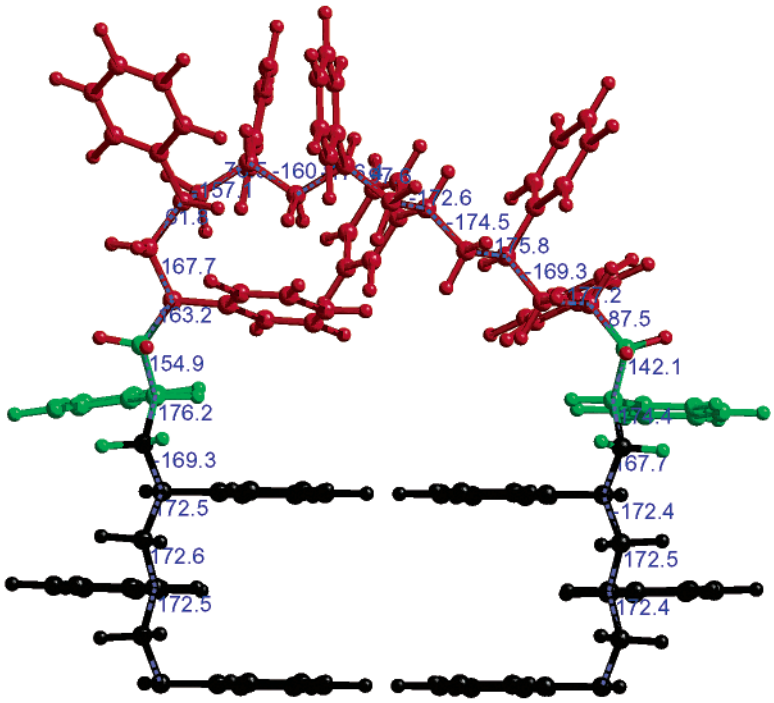

Figure 7. Projection in a plane parallel to the *c* axis of the refined fold *3*73 obtained by the MM2_85 force field, with the indication of the values of the torsion angles of the backbone. The atoms of the fold, the atoms of the monomeric units of the starting and of the end stems nearer the fold surface, and the other atoms of the crystal are drawn with red, green, and black color, respectively.

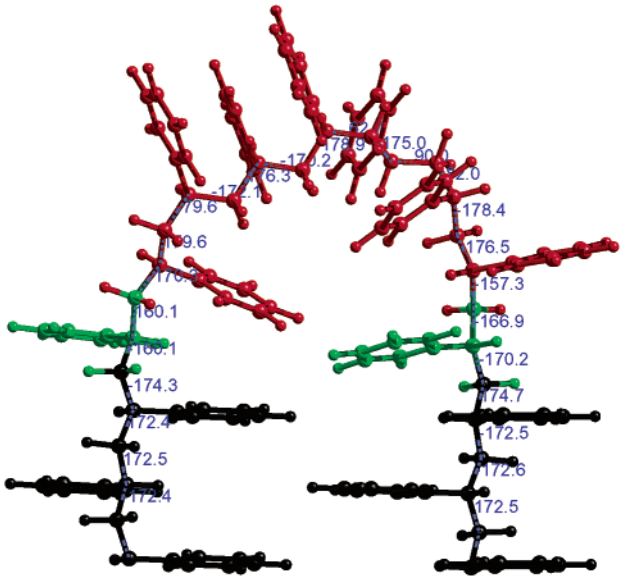

Figure 8. Projection in a plane parallel to the *c* axis of the refined fold *3*′72 obtained by the MM2_85 force field, with the indication of the values of the torsion angles of the backbone. The atoms of the fold, the atoms of the monomeric units of the starting and of the end stems nearer the fold surface, and the other atoms of the crystal are drawn with red, green, and black color, respectively.

refined folds. These adjustments seem significant because the results obtained for the refined folds are generally more consistent with respect to the corresponding results obtained for the optimized folds. At this time this approach is the most complete in considering the factors which determine the adjacent reentry chain folding.

We have calculated, for each force field, the value of E_{fold} as the mean of the lowest values obtained for the various folds. It is included in the range from 46 to 89 kJ/mol of monomeric unit if we consider all the force field. A very similar range (from 50 to 85 kJ/mol of monomeric unit) was obtained for the for the β form of sPS.[30] These results indicate that the energy required to fold a chain of sPS in due prevailingly to the constitution and configuration of the polymer chains rather than to the packing of the chains.

Acknowledgment. The authors are grateful to the Ministero della Università e della Ricerca Scientifica (Italy), PRIN 2000, for the financial support.

References and Notes

(1) Ishihara, N.; Seimiya, T.; Kuramoto, M.; Uoi, M. *Macromolecules* **1986**, *19*, 2464.
(2) Zambelli, A.; Longo, P.; Pellecchia, C.; Grassi, A. *Macromolecules* **1987**, *20*, 2035.
(3) Ishihara, N.; Kuramoto, M.; Uoi, M. *Macromolecules* **1988**, *21*, 3356.
(4) Immirzi, A.; de Candia, F.; Iannelli, P.; Zambelli, A.; Vittoria, V. *Makromol. Chem. Rapid Commun.* **1988**, *9*, 761.
(5) Guerra, G.; Vitagliano, V. M.; De Rosa, C.; Petraccone, V.; Corradini, P. *Macromolecules* **1990**, *23*, 1539.
(6) Corradini, P.; Napolitano, R.; Pirozzi, B. *Eur. Polym. J.* **1990**, *26*, 157.
(7) Woo, E. M.; Sun, Y. S.; Yang, C. P. *Prog. Polym. Sci.* **2001**, *26*, 945.
(8) Greis, O.; Xu, Y.; Asano, T.; Petermann, J. *Polymer* **1989**, *30*, 590.
(9) De Rosa, C.; Guerra, G.; Petraccone, V.; Corradini, P. *Polym. J.* **1991**, *23*, 1435.
(10) Corradini, P.; De Rosa, C.; Guerra, G.; Napolitano, R.; Petraccone, V.; Pirozzi, B. *Eur. Polym. J.* **1994**, *30*, 1173.
(11) De Rosa, C. *Macromolecules* **1996**, *29*, 8460.
(12) Cartier, L.; Okihara, T.; Lotz, B. *Macromolecules* **1998**, *31*, 3303.
(13) De Rosa, C.; Rapacciuolo, M.; Guerra, G.; Petraccone, V.; Corradini, P. *Polymer* **1992**, *33*, 1423.
(14) Chatani, Y.; Shimane, Y.; Ijitsu, T.; Yukinari, T. *Polymer* **1993**, *34*, 1625.
(15) Chatani, Y.; Shimane, Y.; Inoue, Y.; Inagaki, T.; Ishioka, T.; Ijitsu, T.; Yukinari, T. *Polymer* **1992**, *33*, 488.
(16) De Rosa, C.; Guerra, G.; Petraccone, V.; Pirozzi, B. *Macromolecules* **1997**, *30*, 4147.

(17) Chatani, Y.; Shimane, Y.; Inagaki, T.; Ijitsu, T.; Yukinari, T.; Shikuma, H. *Polymer* **1993**, *34*, 1620.
(18) Chatani, Y.; Inagaki, T.; Shimane, Y.; Shikuma, H. *Polymer* **1993**, *34*, 4841.
(19) De Rosa, C.; Rizzo, P.; Ruiz de Ballestreros, O.; Petraccone, V.; Guerra, G. *Polymer* **1999**, *40*, 2103.
(20) Bu, W.; Li, Y.; He, J.; Zeng, J. *Macromolecules* **1999**, *32*, 7224.
(21) Ho, R. M.; Lin, C. P.; Tsai, H. Y.; Woo, E. M. *Macromolecules* **2000**, *33*, 6517.
(22) Sun, Y. S.; Woo, E. M. *J. Polym. Sci., Polym. Phys. Ed.* **2000**, *38*, 3210.
(23) Sun, Y. S.; Woo, E. M. *Polymer* **2001**, *42*, 2241.
(24) Ho, R. M.; Lin, C. P.; Hseih, P. Y.; Chung, T. M.; Tsai, H. Y. *Macromolecules* **2001**, *34*, 6727.
(25) Oyama, T.; Shiokawa, K.; Ishimaru, T. *J. Macromol. Sci.* **1973**, *B8*, 229.
(26) Davé, R. S.; Farmer, B. L. *Polymer* **1988**, *29*, 1544.
(27) Schmieg, C.; Grossmann, H. P.; Hägele, P. C. *Polymer* **1990**, *31*, 631.
(28) Napolitano, R.; Pirozzi, B. *Macromolecules* **1998**, *31*, 3626.
(29) Napolitano, R.; Pirozzi, B. *Macromol. Theory Simul.* **2001**, *10*, 532.
(30) Napolitano, R.; Pirozzi, B. *Macromol. Theory Simul.* **2002**, *11*, 472.
(31) Rappé, A. K.; Casewit, C. J.; Colwell, K. S.; Goddard III, W. A.; Skiff, W. M. *J. Am. Chem. Soc.* **1992**, *114*, 10024.
(32) Root, D. M.; Landis, C. R.; Cleveland, T. *J. Am. Chem. Soc.* **1993**, *115*, 4201.
(33) Mayo, S. M.; Olafson, B. D.; Goddard III, W. A. *J. Phys. Chem.* **1990**, *94*, 8897.
(34) Allinger, N. L. *J. Am. Chem. Soc.* **1977**, *99*, 8127.
(35) Sun, H. *J. Phys. Chem. B* **1998**, *102*, 7338.
(36) Rappé, A. K.; Goddard III, W. A. *J. Phys. Chem.* **1991**, *95*, 3358.
(37) Gasteiger, J.; Marsili, M. *Tetrahedron* **1980**, *36*, 3219.
(38) IUPAC Commission on Nomenclature. *Pure Appl. Chem.* **1981**, *53*, 733.
(39) Napolitano, R.; Pirozzi, B. *Macromolecules* **1993**, *26*, 7225.

MA021588S